

Numerical Analysis Of A Radio Frequency-Assisted Convective Drying

Ahmet Kaya

Abstract: A two-dimensional analysis of heat and mass transfer during radio-frequency assisted convective drying of a rectangular apple slice is performed using an implicit finite difference method. Temperature and moisture distributions inside the object are predicted. Effects of level of power density and heat transfer coefficient on moisture and temperature profiles in the product are evaluated. It is shown that increasing the level of power density and heat transfer coefficient increase the temperature and decrease the moisture in the product. The results obtained from the present model are compared with those available the literature and a considerably good agreement is found.

Keywords: Convective drying, Numerical Solution, Finite difference, ADI, Radio frequency, Temperature distribution, Moisture distribution.

1 INTRODUCTION

DRYING is a highly energy-intensive process and the total cost of drying is largely determined by the cost of energy that can be minimized by the application of a maximum-efficiency heating technique [1,2]. In order to enhance heat and mass transfer during drying, to preserve quality and to minimize energy consumption, a substantial amount of research has been focused on innovative heating and drying processes [2]. Radio frequency (RF) heating is an emerging technology which has been used for food processing [3], drying [4,5] and thermal therapy [6]. Contrary to conventional heating methods where heat is transferred from a heating medium to a product, in RF heating a volumetric heat generation takes place inside the product due to the interaction between RF waves and the product molecules [7]. RF heating offers several distinct advantages over convective heating, such as, shorter heating times, uniform heating throughout the material, lower temperature drying because the RF energy heats the water (the dielectric) contained in the product with less heating of the base material, moisture profiling or leveling to create more consistent product quality, efficient energy conversion, better and more rapid process control, and fewer environmental problems [8]. RF heating also has some limitations. It is not useful for irregularly shaped products because it might not heat complex shapes uniformly, it is generally not effective with organic solvents, and drying with RF alone can be very expensive in terms of both equipment and operating costs [2]. Combined RF and convection drying has been the subject of a number of investigations. Based on experimental data and analysis of the heat and mass transfer mechanisms, Jumah [2] presented theoretical analysis based on the simultaneous heat and mass transfer for the radio frequency-assisted fluidized bed drying of particulates. Corn was chosen as a test material. Two radio frequencies heating schemes, continuous and intermittent, were distinguished and tested. Numerical results show that the moisture distribution inside the corn had a significant effect on the RF drying kinetics. Ptasznik et al. [9] developed a semi-empirical model for RF-assisted convective drying of shrinkable and hygroscopic materials with internal resistance to mass transfer.

Simulation results indicate that internal heat generation strongly affects both the product temperature and drying kinetics. Dostie [10] performed a numerical and experimental study on the drying of mineral board using infrared, RF and convection. Some characteristics were identified and used to optimize the application of these drying techniques for this specific product. A study of the operation of a draught tube spouted bed in conjunction with dielectric heat was carried out by Colley [11]. The addition of radio frequency allowed a greater amount of energy to be input into the particulate material in a given time, increasing the drying rate; however, the drying pattern was unaffected by the ratio of the RF to convective heat addition. Poulin et al. [12] conducted a thorough study of the combined convection and RF drying process. The results indicate that the analogy between heat and mass transfer was valid in the combined convection and RF conditions studied. Experimental results have showed that the moisture distribution inside the product has a significant effect on the RF drying kinetics. Marshall and Metaxas [13] developed and validated a boundary value approach to model the RF electric field strength during the RF-assisted heat pump drying of particulate materials. The results show that the combined system improves the dryer and heat pump performance. Koumoutsakos et al. [14] developed a one-dimensional mathematical model to describe the transport phenomena during continuous radio frequency/vacuum (RF/V) drying of thick lumber. The controlling resistances and transport mechanisms during RF/V wood drying was discussed and compared against those in convective drying. They found that increasing the internal heat generating source term increased the temperature and decreased the moisture content in the product. Most of the above studies on radio frequency assisted convective drying is either experimental or one dimensional numerical study. The objectives of this study are: (1) to develop a mathematical model of RF-assisted convective; (2) to investigate the effects of the levels of power densities and heat transfer coefficient on the temperature and moisture profile in the product.

2 THEORETICAL ANALYSIS

In this section, a numerical procedure was developed to analyze heat and mass transfer through diffusion for radio-frequency assisted convective drying with some assumptions: (i) thermophysical properties of the material are constant, (ii) negligible shrinkage or deformation of the material during drying, and (iii) negligible radiation effects. It is also included radio frequency heating effect in the energy equation. Under

- Ahmet Kaya, Department of Mechanical Engineering, Kahramanmaraş Sutcu Imam University, 46100 Kahramanmaraş, TURKEY
E-mail: ekaya38@gmail.com

the above assumptions, the following governing 2-D heat and moisture transfer equations can be written:

$$\rho c_p \frac{\partial T}{\partial t} = k \left(\frac{\partial^2 T}{\partial x^2} + \frac{\partial^2 T}{\partial y^2} \right) + \Phi \tag{1}$$

$$\frac{\partial M}{\partial t} = D \left(\frac{\partial^2 M}{\partial x^2} + \frac{\partial^2 M}{\partial y^2} \right) \tag{2}$$

The volumetric heat source term represents the effect of Radio frequency (RF) heating. When $\epsilon'' = 0$, this model reduces to the conventional convective drying. The RF power dissipation within the material is related to the electric field strength within the material E and the dielectric properties of the material by the following equation [2]:

$$\Phi = (5.56 \times 10^{-11}) E^2 f \epsilon'' \tag{3}$$

where f (Hz) is the frequency, and ϵ'' is the dielectric loss factor of the material. The initial and boundary conditions for heat transfer are given as follows:

$$T(x, y, 0) = T_i \tag{4}$$

$$\left. \begin{aligned} k \frac{\partial T(0, y, t)}{\partial x} + h_{fg} h_m (M - M_d) &= h(T - T_d) \text{ at } x=0 \text{ and } 0 \leq y \leq H \\ -k \frac{\partial T(L, y, t)}{\partial x} + h_{fg} h_m (M - M_d) &= h(T - T_d) \text{ at } x=L \text{ and } 0 \leq y \leq H \\ k \frac{\partial T(x, 0, t)}{\partial y} + h_{fg} h_m (M - M_d) &= h(T - T_d) \text{ at } y=0 \text{ and } 0 \leq x \leq L \\ -k \frac{\partial T(x, H, t)}{\partial y} + h_{fg} h_m (M - M_d) &= h(T - T_d) \text{ at } y=H \text{ and } 0 \leq x \leq L \end{aligned} \right\} \tag{5}$$

And for moisture transfer;

$$M(x, y, 0) = M_i \tag{6}$$

$$\left. \begin{aligned} -D \frac{\partial M(0, y, t)}{\partial x} &= h_m (M - M_d) \text{ at } x=0 \text{ and } 0 \leq y \leq H \\ D \frac{\partial M(L, y, t)}{\partial x} &= h_m (M - M_d) \text{ at } x=L \text{ and } 0 \leq y \leq H \\ -D \frac{\partial M(x, 0, t)}{\partial y} &= h_m (M - M_d) \text{ at } y=0 \text{ and } 0 \leq x \leq L \\ D \frac{\partial M(x, H, t)}{\partial y} &= h_m (M - M_d) \text{ at } y=H \text{ and } 0 \leq x \leq L \end{aligned} \right\} \tag{7}$$

3 SOLUTION METHODOLOGY

The heat and mass transfer equations in the rectangular object have been developed in the previous section are coupled, non-linear and unsteady. The equations are solved numerically by using finite difference method with alternating direction implicit method (ADI) [15] algorithm applied to two-dimensional cartesian coordinate together with boundary and initial conditions. The most attractive feature of this method is that

the solution converges fast [16]. Suppose the computations are to be advanced from the (n)th time level to the (n+1)th time level. The simple implicit method is used for one of the directions, say x, and the simple explicit method is used for the other direction, i.e. y. Then, the advancement from the (n+1)th level is done by reversing the directions of the implicit and explicit methods. The computational procedure is continued by alternately changing the directions of the explicit and implicit methods [17]. The application of the ADI method for discretization of Eq.1 is illustrated as follows. Suppose the implicit scheme is used in the x-direction and the explicit scheme in the y-direction to advance from the nth to the (n+1)th time level. The finite difference approximation of Eq.1 is given by

$$\left. \begin{aligned} \frac{T_{i,j}^{n+1} - T_{i,j}^n}{\Delta t} &= \frac{T_{i+1,j}^{n+1} + T_{i-1,j}^{n+1} - 2T_{i,j}^{n+1}}{(\Delta x)^2} \\ &+ \frac{T_{i,j+1}^n + T_{i,j-1}^n - 2T_{i,j}^n}{(\Delta y)^2} + \frac{1}{k} \phi_{i,j}^{n+1} \end{aligned} \right\} \tag{8}$$

For the next time level, an explicit formulation is used for the x-direction and an implicit formulation for the y-direction. Then the finite difference approximation for Eq.1 from the (n+1)th to the (n+2)nd time step becomes

$$\left. \begin{aligned} \frac{T_{i,j}^{n+2} - T_{i,j}^{n+1}}{\Delta t} &= \frac{T_{i+1,j}^{n+1} + T_{i-1,j}^{n+1} - 2T_{i,j}^{n+1}}{(\Delta x)^2} \\ &+ \frac{T_{i,j+1}^{n+2} + T_{i,j-1}^{n+2} - 2T_{i,j}^{n+2}}{(\Delta y)^2} + \frac{1}{k} \phi_{i,j}^{n+1} \end{aligned} \right\} \tag{9}$$

This equation utilizes the results from the previous time level n+1 to calculate the temperatures at the time level n+2 [17]. For computational purposes, it is convenient to rearrange Eqs. (8) and (9) such that at each time level, the unknown quantities appear on one side of the equality, say, on the left and known quantities on the other side i.e., on the right. Equations (8) and (9), respectively, become [17]

$$\left. \begin{aligned} -r_x T_{i-1,j}^{n+1} + (1+2r_x) T_{i,j}^{n+1} - r_x T_{i+1,j}^{n+1} &= \\ = r_y T_{i,j-1}^n + (1-2r_y) T_{i+1,j}^n + r_y T_{i+1,j}^n + \frac{\alpha \Delta t}{k} \Phi_{i,j}^{n+1} \end{aligned} \right\} \tag{10}$$

for the time level n+1, and

$$\left. \begin{aligned} -r_y T_{i,j-1}^{n+2} + (1+2r_y) T_{i,j}^{n+2} - r_y T_{i,j+1}^{n+2} &= \\ = r_x T_{i-1,j}^{n+1} + (1-2r_x) T_{i,j}^{n+1} + r_x T_{i+1,j}^{n+1} + \frac{\alpha \Delta t}{k} \Phi_{i,j}^{n+2} \end{aligned} \right\} \tag{11}$$

for the level n+2, where

$$r_x = \frac{\alpha \Delta t}{(\Delta x)^2} \text{ and } r_y = \frac{\alpha \Delta t}{(\Delta y)^2} \tag{12}$$

When solving the problem, Eqs. (10) and (11) are repeated alternatively. The advantage of this approach over the fully implicit or Crank-Nicolson methods is that, each equation, although implicit, is only tridiagonal [17]. Readers are referred to Ozisik [17] for the details of the numerical methods. Initial and boundary conditions are;

$$T_{i,j,0} = T_i \quad (13)$$

for x-direction

$$\left. \begin{aligned} \left(\frac{k}{\Delta x} + h \right) T_{0,j}^{n+2} + \left(-\frac{k}{\Delta x} \right) T_{i,j}^{n+1} &= \\ = hT_d + h_m h_{fg} (M_{0,j}^{n+1} - M_d) \end{aligned} \right\} \quad (14)$$

And

$$\left. \begin{aligned} \left(-\frac{k}{\Delta x} \right) T_{N-1,j}^{n+1} + \left(\frac{k}{\Delta x} + h \right) T_{N,j}^{n+1} &= \\ = hT_d + h_m h_{fg} (M_{N,j}^{n+1} - M_d) \end{aligned} \right\} \quad (15)$$

for the y-direction

$$\left. \begin{aligned} \left(\frac{k}{\Delta y} + h \right) T_{i,0}^{n+2} + \left(-\frac{k}{\Delta y} \right) T_{i,1}^{n+2} &= \\ = hT_d + h_m h_{fg} (M_{i,0}^{n+2} - M_d) \end{aligned} \right\} \quad (16)$$

And

$$\left. \begin{aligned} \left(-\frac{k}{\Delta y} + h \right) T_{i,m-1}^{n+2} + \left(\frac{k}{\Delta y} + h \right) T_{i,m}^{n+2} &= \\ = hT_d + h_m h_{fg} (M_{i,m}^{n+2} - M_d) \end{aligned} \right\} \quad (17)$$

Discretization of the mass transfer equation (Eq.2) and initial and boundary conditions have similar process to Eqs.(8), (9) and (13-17). The above difference equations are solved to obtain temperature and moisture distributions inside the slab object at different time periods. In order to prevent the divergence, an underrelaxation parameter is introduced into the heat and mass transfer equations, and its optimum value for both equations is shown to be 0.5. Starting from the initial condition and choosing a suitable time interval, this is continued until steady-state solution exists. The object is discretized by 31 x 31 of mesh size. The results obtained with this size of the mesh are observed to deviate negligibly from those obtained by a 61 x 61 mesh size. Therefore, a 31 x 31 is used for the object [18].

4 RESULTS AND DISCUSSION

This section presents the temperature and moisture distribution inside a rectangular product of dimensions 0.05 m x 0.05 m. The object considered in the simulation was a rectangular-shaped apple. Thermophysical properties and the

drying conditions used in the simulation are tabulated in Table 1. In order to study the effect of the level of power and heat transfer coefficient, the following values of the level of power, and heat transfer coefficient h, are used: 0, 1000, 2500 and 5000 W/m³ and 25, 50, 75 and 100 W/m²K, respectively. In order to investigate the accuracy of the model predictions, the numerical solution results have been compared with those given in another numerical study [19] and the results are given in Figure 1. A pure convective drying (i.e., =0 W/m³) version of the above model is employed for validation purposes. Temperature and moisture profiles are compared at 200 s and excellent agreements have been observed (Figure 1 (a) and (b)). Also, the predicted center temperature and moisture distributions inside the rectangular object are compared with experimental [20] and numerical [19] data available in the literature and are shown in Fig. 2. Experimental drying conditions and product properties are listed in Table 2. As it is seen from Figs. 1 and 2 excellent agreements have been observed.

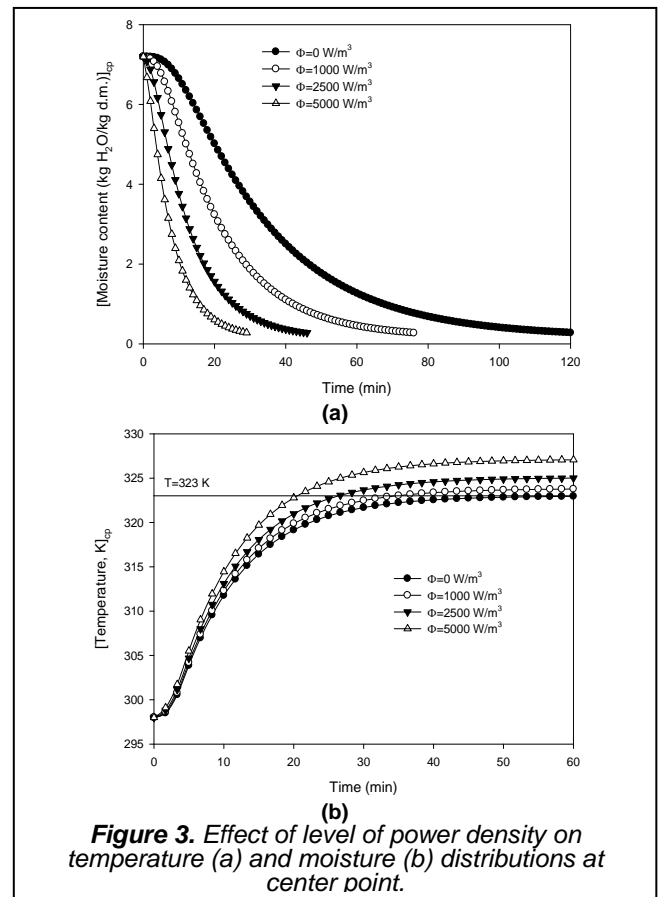
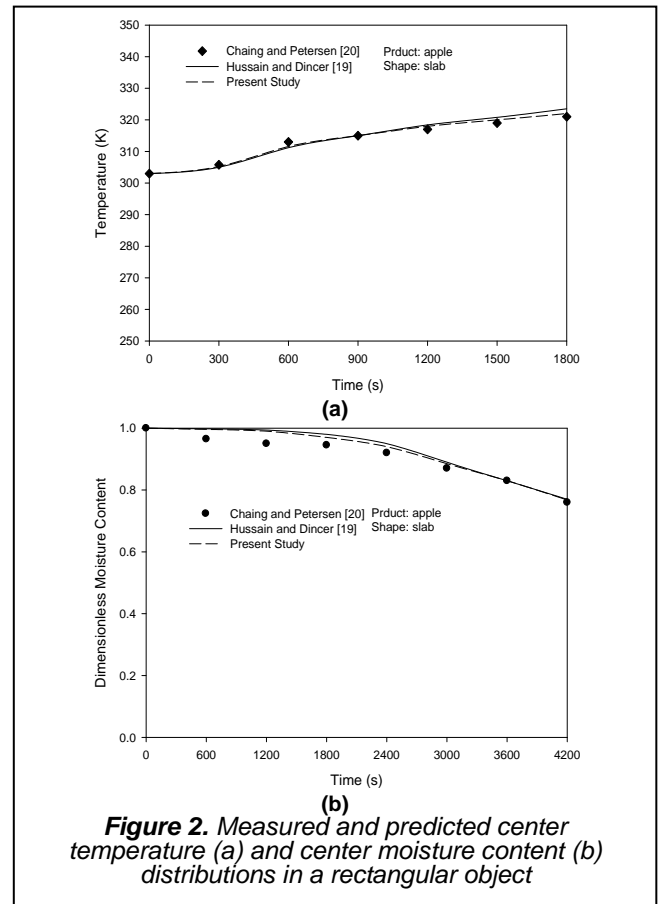
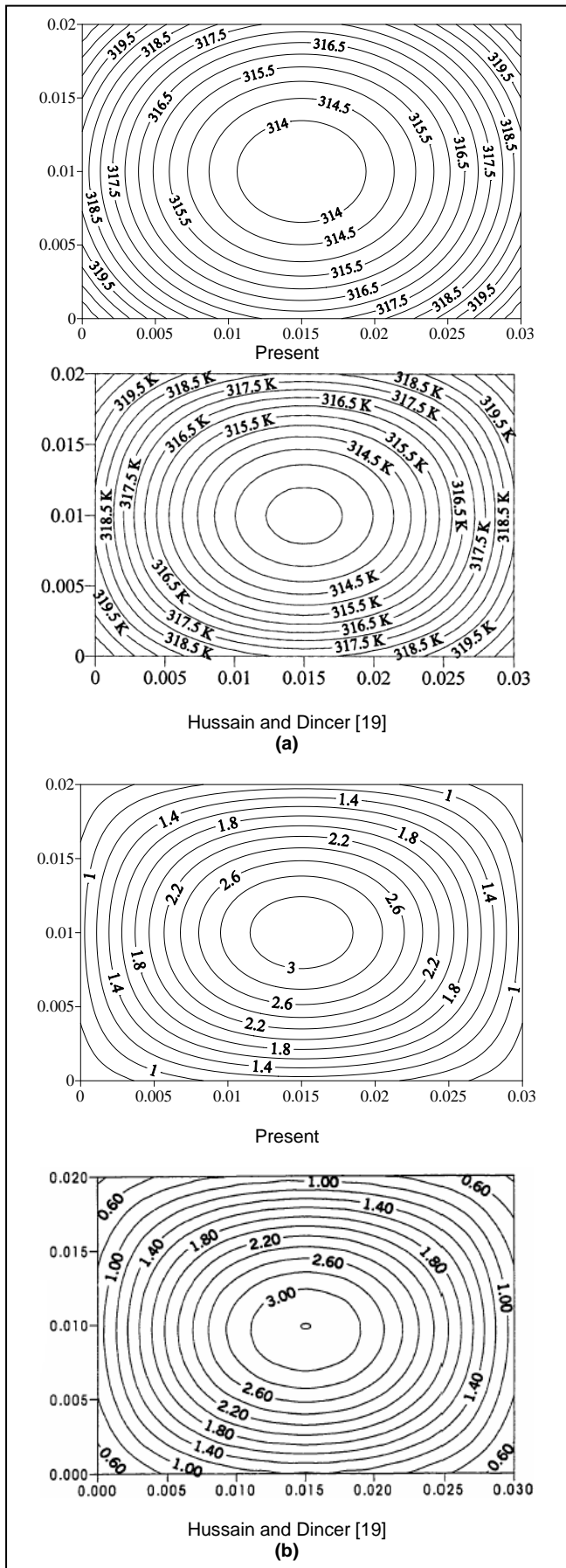
Table 1. Thermophysical properties and drying conditions used in the simulation

K	0.576 W/mK
ρ	856 kg/m ³
c_p	1929.72 J/kg K
h_m	0.0001 m/s
h_{fg}	2438 kJ/kgK
T_d	323 K
T_i	298 K
M_i	7.196 g/g (db)
RH	0.196 g/g (db)
Reference	Hussain and Dincer [19]

Figure 3 shows the drying (a) and temperature (b) curves for different levels of power densities. The RF heating simultaneously with convective drying significantly increases the drying rate, as evidenced by a significant reduction in drying time (Figure 3(a)) compared to pure convective drying (=0 W/m³). In conventional heating, internal thermal penetration is slow, and this slows down the drying process.

Table 2. Experimental drying conditions and product properties

Object	Rectangular-shaped apple
Size	4.8 x 4.9 x 2.0 cm
k	0.148+0.493 x Mi (W/mK)
ρ	856 kg/m ³
c_p	(1.4+3.22 x Mi) x 1000 (J/kg K)
T_d	354 K
T_i	303 K
M_i	87%
RH	12%
References	Hussain and Dincer [19] and Chiang and Petersen [20]



In RF-assisted convective drying, on the other hand, electromagnetic energy penetrates easily through the dry surface layer and is absorbed selectively in the wet core, where a higher rate of heating is desired [2]. Figure 3 (b) shows the variation of temperature with drying time at center point. Increase of the power causes an increase in the temperature everywhere. As a result, product temperature increases with a rate much greater than pure convective heating ($h=0 \text{ W/m}^2$). Similar results were given by Jumah [2] and Koumoutsakos et al. [14]. Figure 4 (a) and (b) show the variations of center temperature and center moisture content for different heat transfer coefficient. Increasing the heat transfer coefficient increases temperature and decreases moisture content in the product center. The temperature rises rapidly and moisture content decreases for all the heat transfer coefficients in the early heating period due to convective and evaporative boundary conditions.

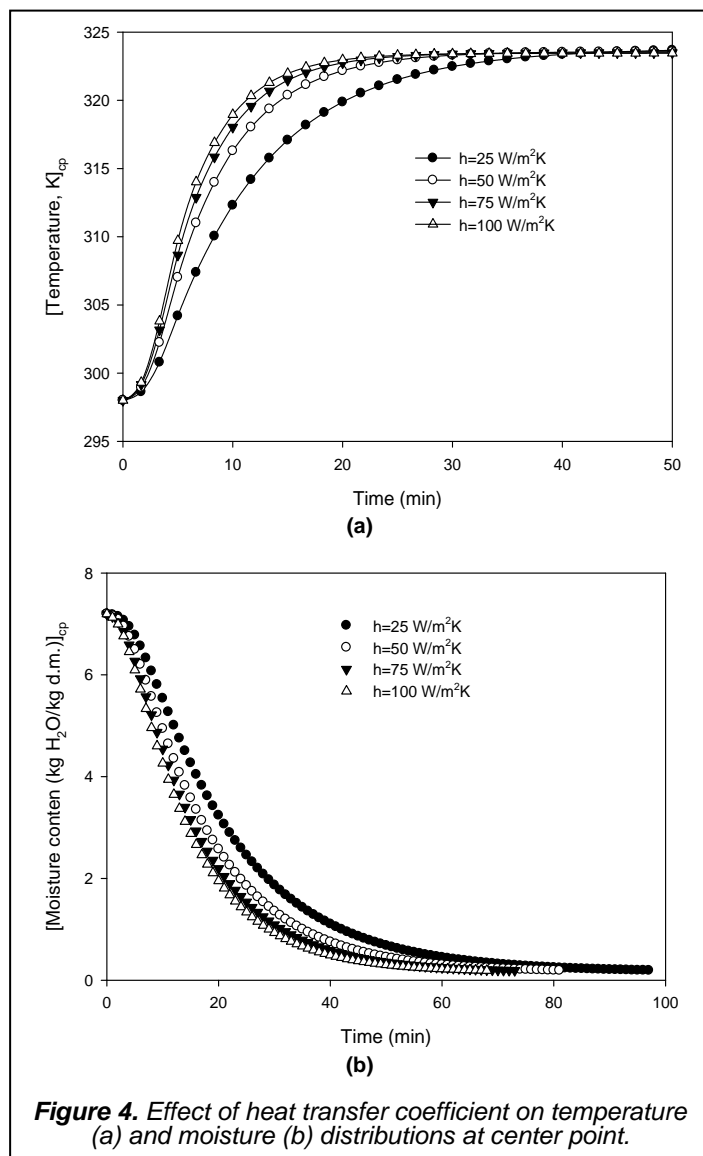


Figure 4. Effect of heat transfer coefficient on temperature (a) and moisture (b) distributions at center point.

moisture distribution in the product for different levels of power densities are shown in Fig. 6 at 500 s. The moisture in the object is reduced as the increasing the levels of power densities.

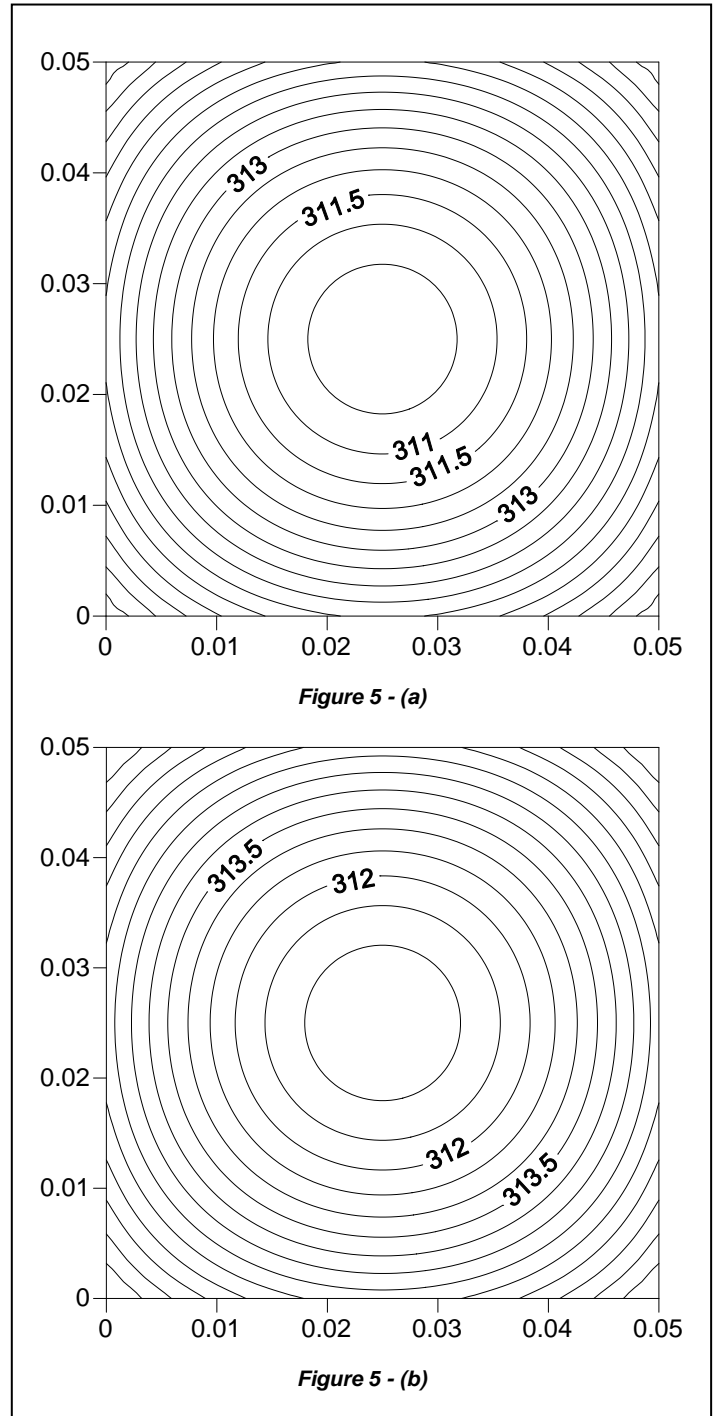
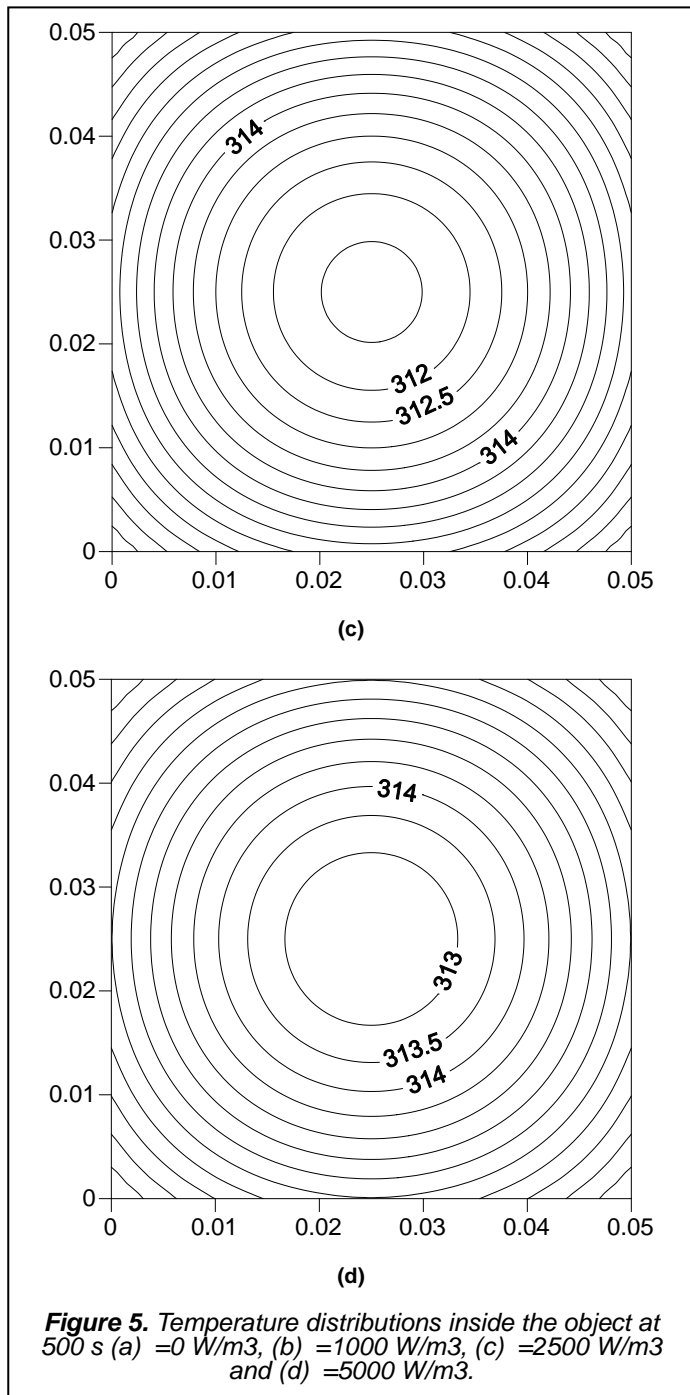
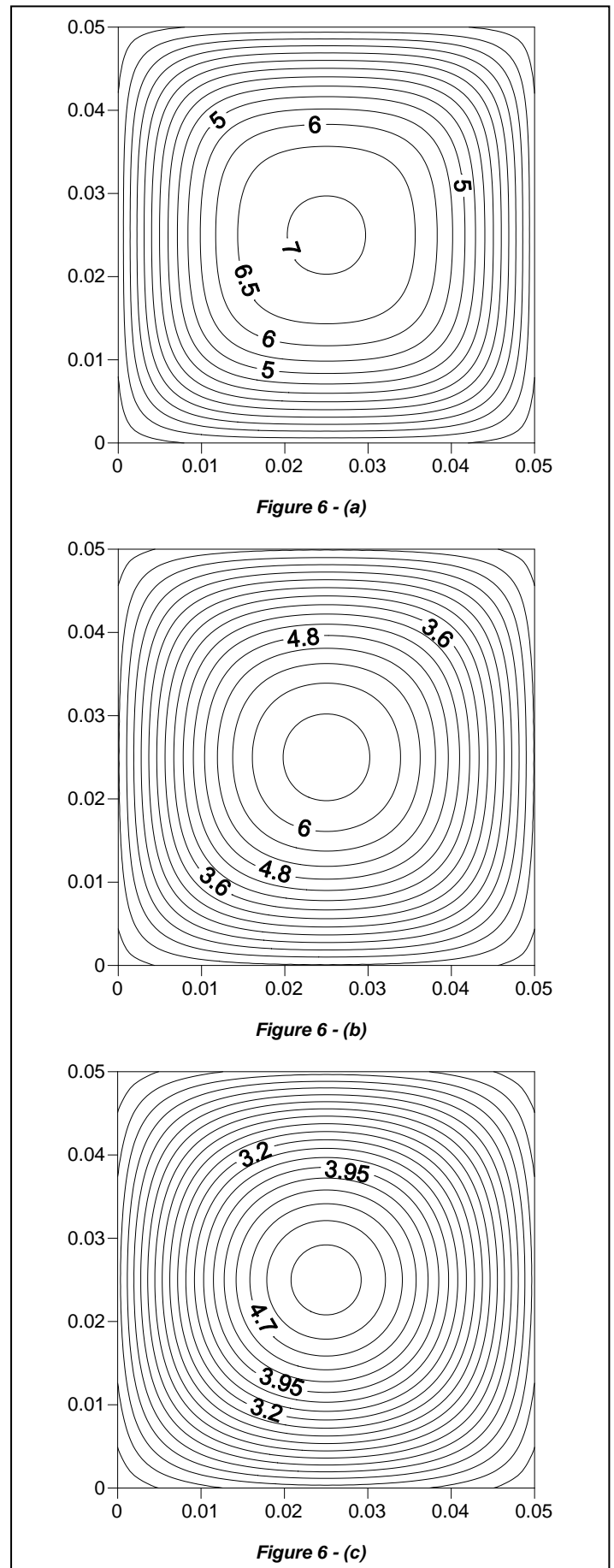


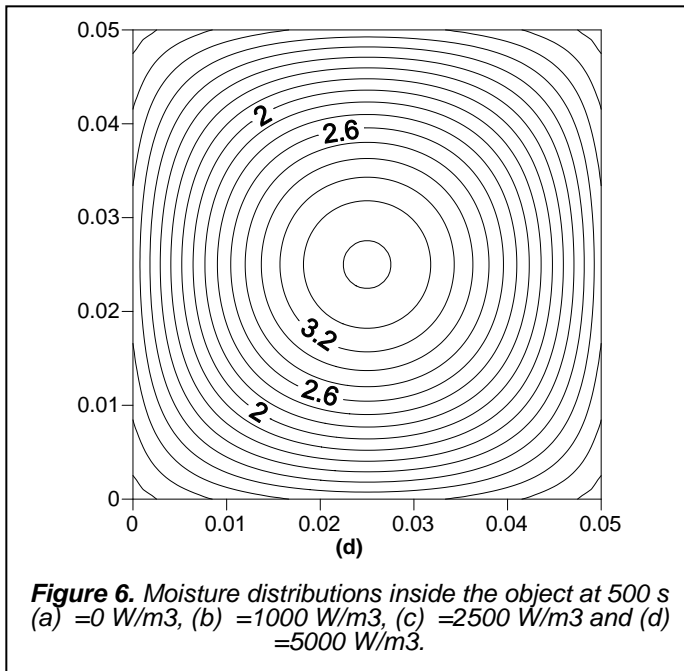
Figure 5 shows the temperature distribution in the product for different levels of power densities at 500 s. Temperature in the object increases as the levels of power densities. Moreover, temperature distribution inside the object is uniform because the moisture diffusivity in the product is taken constant. The



5 CONCLUSION

In this article, the numerical simulation of a RF-assisted convective drying process in a two-dimensional rectangular object is presented. It is found that the temperature and moisture profiles rises with levels of power densities and heat transfer coefficient. Increasing the levels of power densities and heat transfer coefficient increases temperature and decreases moisture in the product because the boundary conditions for heat and mass transfer are coupled. Validation of the results obtained from the present analysis is performed with another numerical study in the literature. A considerably good agreement is found for the temperature and moisture distributions inside the product.





NOMENCLATURE

c_p	constant pressure specific heat, J/kg K
D	moisture diffusivity, m ² /s
E	electric field strength within the material, V/m
f	frequency, Hz
h	heat transfer coefficient, W/m ² K
h_m	moisture transfer coefficient, m/s
H	height, m
H_{fg}	local heat of desorption–vaporization, kJ/kgK
k	thermal conductivity, W/mK
L	length, m
M	moisture content, kg/kg db
S	source term
t	time, s
T	temperature, K
x, y	coordinates

Greek symbols

α	thermal diffusivity, m ² /s
ϵ_0	permittivity of free space, F/m
ϵ''	dielectric loss factor
Φ	volumetric heat generated by RF power, W/m ³
ρ	density, kg/m ³

Subscripts

cp	center point
d	drying air
db	dry base
s	surface

REFERENCES

- [1] C. Strumillo, P. Jones, R. Zylla, "Energy Aspects in Drying", In: *Mujumdar AS (ed) Handbook of Industrial Drying*, 2nd edn, Marcel Dekker, New York, pp 1241–1275, 1995.
- [2] R. Jumah, "Modelling and Simulation of Continuous and Intermittent Radio Frequency-Assisted Fluidized Bed Drying of Grains", *Food Bioprod Process* 83, pp 203–210, 2005.
- [3] J. Houben, L. Schoenmakers, E. Putten, P. Roon, B. Krol, "Radio-Frequency Pasteurization of Sausage Emulsions as A Continuous Process", *J Microw Power Electromagn Energy* 26, pp 202–205, 1991.
- [4] A. Poulin, M. Dostie, P. Proulx, J. Kendall, "Convective Heat and Mass Transfer and Evolution of Moisture Distribution Combined Convection and Radio Frequency Drying", *Dry Technol* 5, pp 1893–1907, 1997.
- [5] P.A. Balakrishnan, N. Vedaraman, V.J. Sunder, C. Muralidharan, S. Swaminathan, "Radio Frequency Heating—A Prospective Leather Drying System for Future", *Dry Technol* 22, pp 1969–1982, 2004.
- [6] B. Maurizio, C. Giovanni, G. Mirko, P. Giancarlo, L. Giuseppe, O. Riccardo, "Radio Frequency (RF) Ablation of Renal Tumours Does Not Produce Complete Tumour Destruction: Results of A Phase II Study", *Eur Urol Suppl* 3, pp 14–17, 2004.
- [7] M. Izadifar, O.D. Baik, G.S. Mittal, "Radio Frequency-Assisted Extraction of Podophyllotoxin: Prototyping of Packed Bed Extraction Reactors and Experimental Observations", *Chem Eng Process* 48, pp 1437–1444, 2009.
- [8] R.F. Schiffmann, "Microwave and Dielectric Drying", In: *Mujumdar AS (ed) Handbook of Industrial Drying*, 2nd edn. Marcel Dekker, New York, pp 373–454, 1995.
- [9] W. Ptaszniak, S. Zygmunt, T. Kudra, "Simulation of Rf-Assisted Convective Drying of Seed Quality Broad Beans", *Dry Technol* 8, pp 977–992, 1990.
- [10] M. Dostie, "Optimization of A Drying Process Using Infrared, Radio Frequency and Convection Heating", In: *Mujumdar AS (ed) Drying'92*, Elsevier, Amsterdam, pp 679–684, 1992.
- [11] M.I. Colley, "Radio Frequency Enhanced Draught Tube Spouted Bed Dryer", *Dry Technol* 11, pp 355–368, 1993.
- [12] A. Poulin, M. Dostie, P. Proulx, J. Kendall, "Convective Heat and Mass Transfer and Evolution of The Moisture Distribution in Combined Convection and Radio Frequency Drying", In: *Mujumdar AS (ed) Drying'96*, Elsevier, Amsterdam, pp 195–204, 1996.
- [13] M.G. Marshall, A.C. Metaxas, "A Novel Radio Frequency Assisted Heat Pump Dryer", *Dry Technol* 17, pp 1571–1578, 1999.
- [14] A. Koumoutsakos, S. Avramidis, S.G. Hatzikiriakos, "Radio Frequency Vacuum Drying of Wood; I. Mathematical Model", *Dry Technol* 19(1), pp 65–84, 2001.
- [15] D. Peaceman, H. Rachford, "The Numerical Solution of Parabolic and Elliptic Equations", *J Soc Indust Appl Math*

3, pp 28–41, 1955.

- [16] J.P. Sitompul, I. Istadi, “Alternating Direction Implicit Method for Solving Equations of 2-D Heterogeneous Model of Deep-Bed Grain Drying”, *Proceedings Institut Teknologi Bandung 32 (1)*, pp 425-433, 2000.
- [17] M.N. Ozisik, “Finite Difference Methods in Heat Transfer”, CRC Press, Boca Raton, Florida, 2000.
- [18] A. Kaya, O. Aydin, I. Dincer, “Numerical Modeling of Heat and Mass Transfer During Forced Convection Drying of Rectangular Moist Objects”, *Int J Heat Mass Trans 49*, pp 3094–3103, 2006.
- [19] M.M. Hussain, I. Dincer, “Numerical Simulation of Two-Dimensional Heat and Moisture Transfer During Drying of A Rectangular Object”, *Numerical Heat Transfer, Part A*, 43, pp 867-878, 2003.
- [20] W.C. Chiang, J.N. Petersen, “Experimental Measurement of Temperature and Moisture Profiles During Apple Drying”, *Dry Technol 5(1)*, pp25-49, 1987.